Electronic Supporting Information

Amorphous Cobalt Oxide Nanowalls as Catalyst and Protection Layers on n-type Silicon for Efficient Photoelectrochemical Water Oxidation

Sol A Lee, [†] *Tae Hyung Lee,* [†] *Changyeon Kim,* [†] *Min-Ju Choi,* [†] *Hoonkee Park,* [†] *Seokhoon Choi,* [†] *Jinwoo Lee,* [‡] *Jihun Oh,* [§] *Soo Young Kim,* [*,‖] *and Ho Won Jang*[*,†]

† Department of Materials Science and Engineering, Research Institute of Advanced Materials, Seoul National University, Seoul 08826, Republic of Korea

‡ Department of Chemical and Biomolecular Engineering, Korea Advanced Institute of Science and Technology, Daejeon 34141, Republic of Korea

§ Graduate School of Energy, Environment, Water and Sustainability, Department of Materials Science and Engineering, Korea Advanced Institute of Science and Technology, Daejeon 34141, Republic of Korea

‖ Department of Materials Science and Engineering, Korea University, Seoul 02841, Republic of Korea

*E-mails: sooyoungkim@korea.ac.kr and hwjang@snu.ac.kr

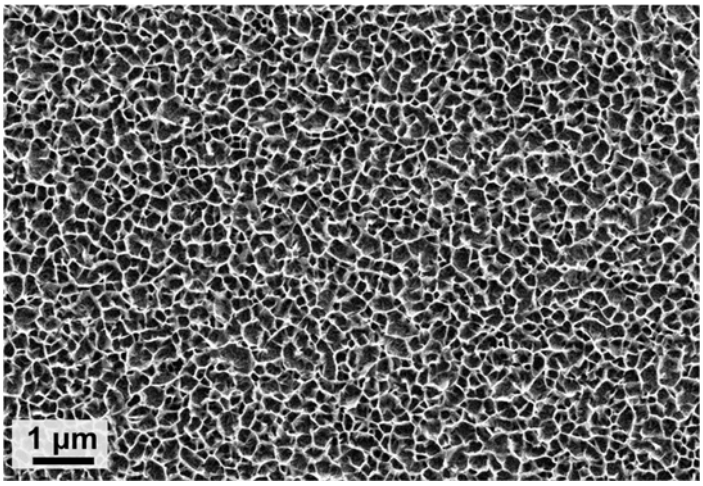

Figure S1. Top view SEM image of the CoO_x NW thin film on n-Si.

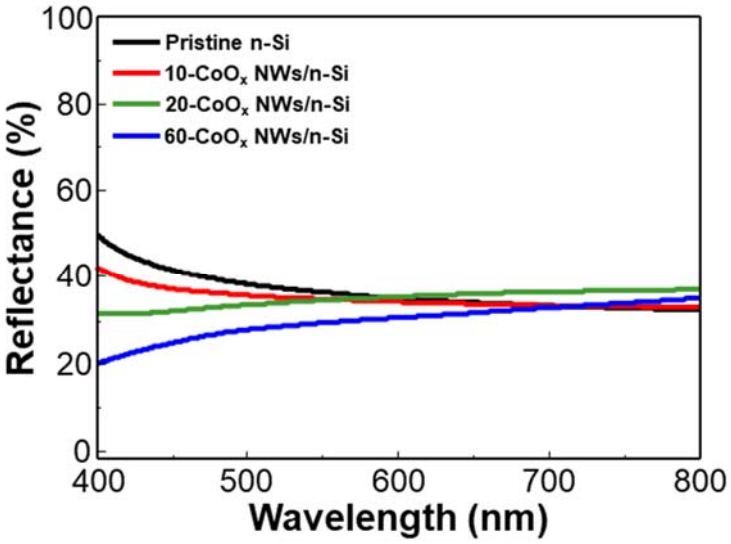

Figure S2. Reflectances of the amorphous CoO_x NW thin films with different thicknesses on silicon.

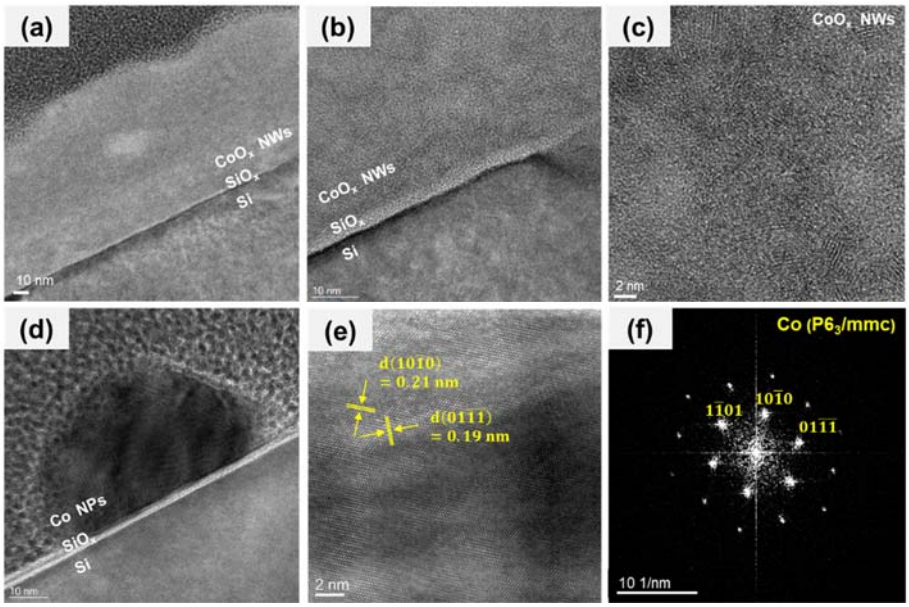

Figure S3. HRTEM images of (a-c) CoO_x NWs/n-Si and (d,e) Co NPs/n-Si. (f) Electron diffraction pattern of Co NPs/n-Si.

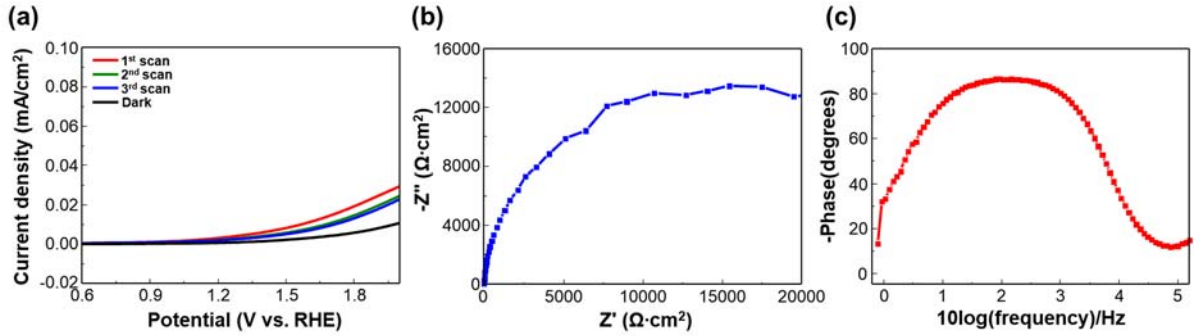

Figure S4. (a) Linear sweep voltammetry of the pristine Si photoanode at a scan rate of 40 mV/s in 1 M NaOH. (b) EIS result of pristine n-Si measured at 1.5 V vs. RHE in 1 M NaOH. (c) Bode plot of pristine n-Si obtained using the curve in (b).

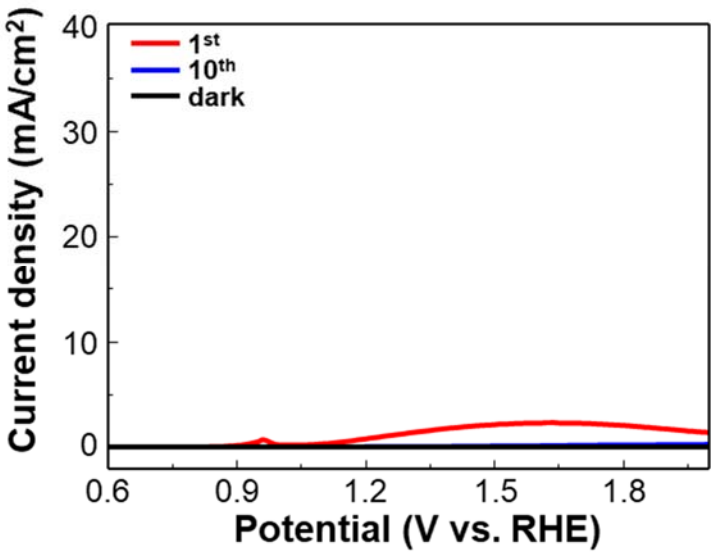

Figure S5. Linear sweep voltammetry of the 1-CoO_x NWs/n-Si photoanode at a scan rate of 40 mV/s in 1 M NaOH.

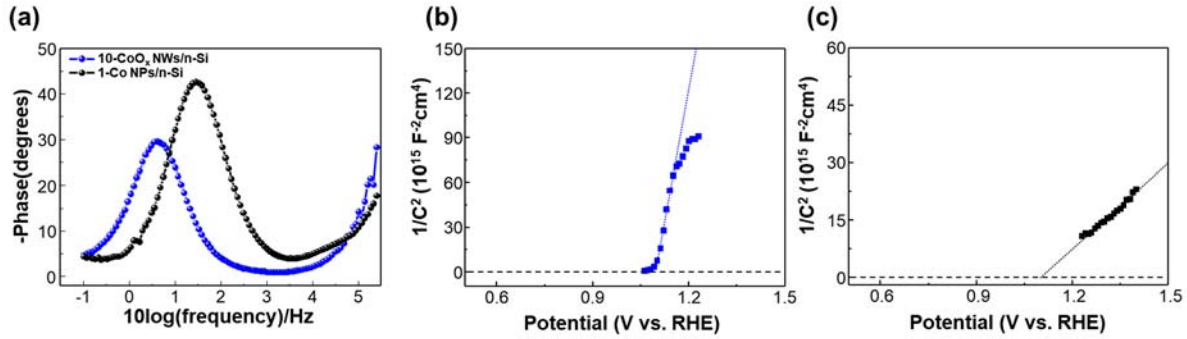

Figure S6. (a) Bode plots of 10-CoO_x NWs/n-Si and 1-Co NPs/n-Si. Mott-Schottky plots of (b) 10-CoO_x NWs/n-Si and (c) 1-Co NPs/n-Si photoanodes measured in 1 M NaOH under light-off condition.

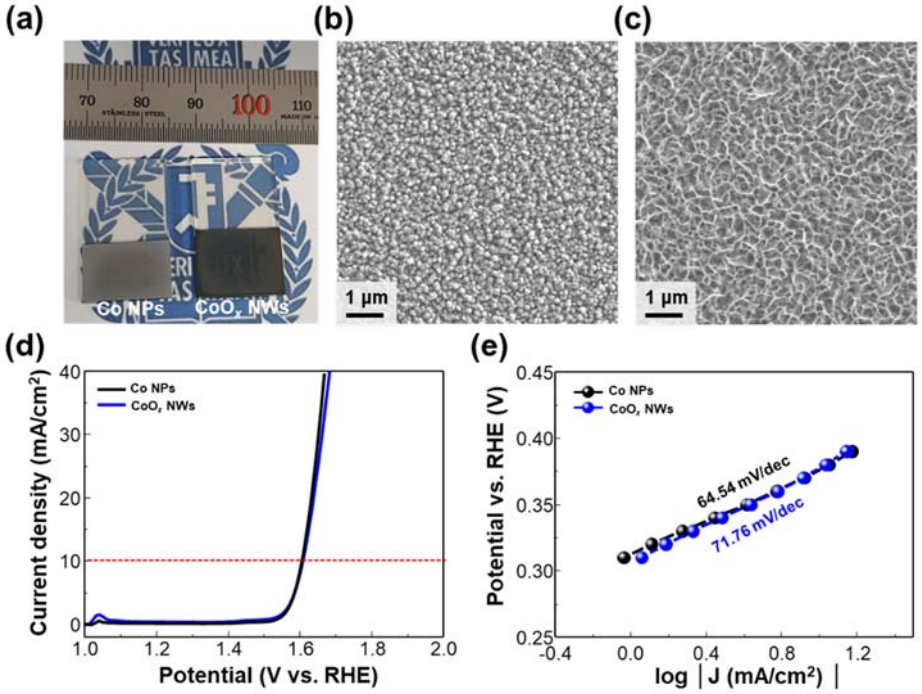

Figure S7. (a) Photographs of electrodeposited 10-Co NPs and 60-CoO_x NW film on FTO substrates. (b-c) SEM images of 10-Co NPs and 60-CoO_x NW film on FTO substrate, respectively. (d) Linear sweep voltammetry of the 10-Co NPs and 60-CoO_x NWs on the FTO substrates at a scan rate of 40 mV/s in 1 M NaOH. (e) Tafel plots obtained using the curves in (d).

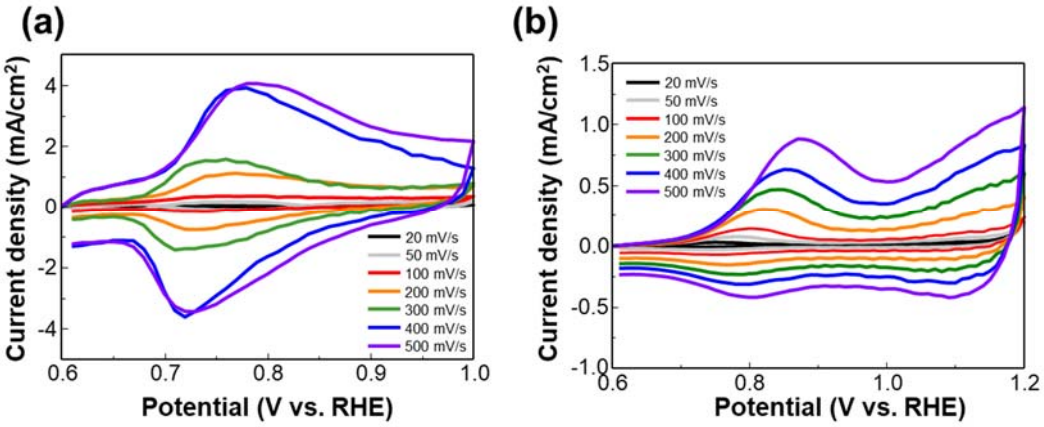

Figure S8. Cyclic voltammograms of the Co^{3+}/Co^{2+} redox wave for the (a) 10-CoO_x NWs/n-Si and (b) 1-Co NPs/n-Si photoanodes under 1 sun illumination (100 mW/cm^2) at different scan rates.

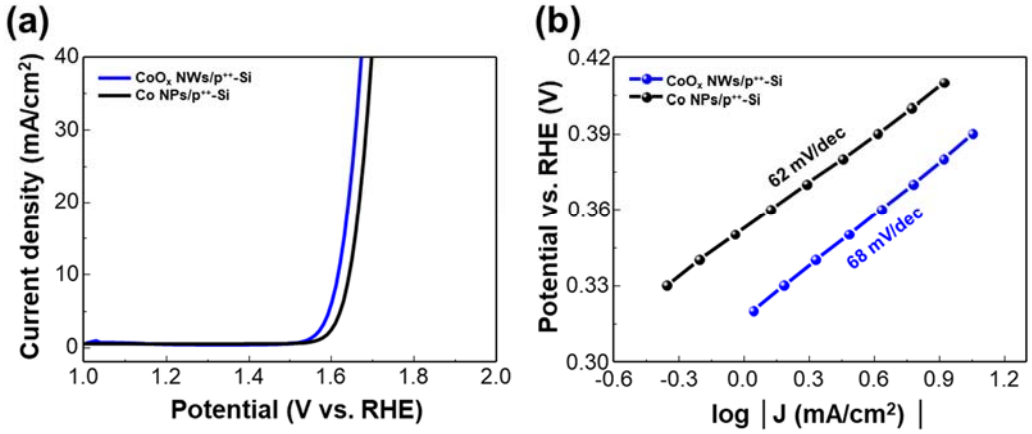

Figure S9. (a) Linear sweep voltammogram of 1-Co NPs and 10-CoO_x NW thin films on the p^{++}-Si substrate at a scan rate of 40 mV/s in 1 M NaOH. (b) Tafel slope of 1-Co NPs/p^{++}-Si and 10-CoO_x NWs/p^{++}-Si in 1 M NaOH.

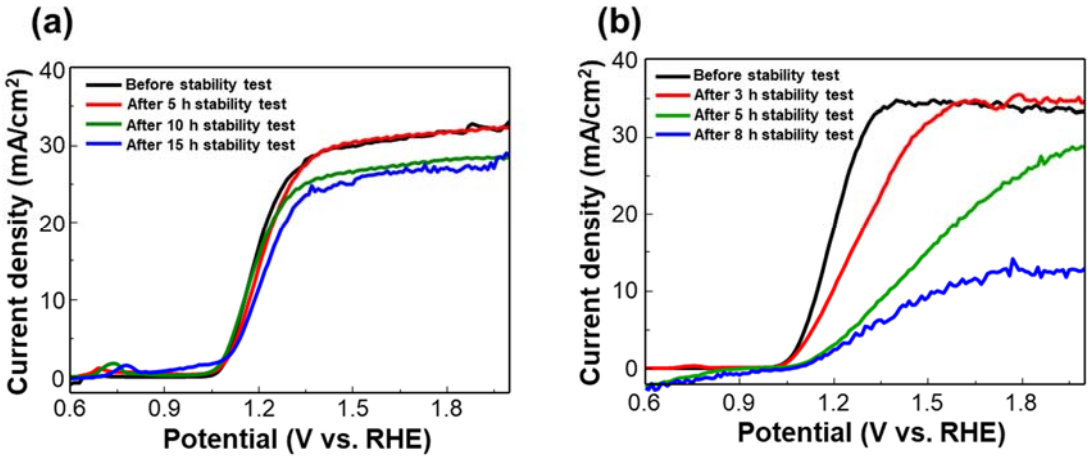

Figure S10. Linear sweep voltammetry of (a) 10-CoO_x/n-Si and (b) 1-Co NPs/n-Si at a 40 mV/s scan rate in 1 M NaOH before and after stability test.

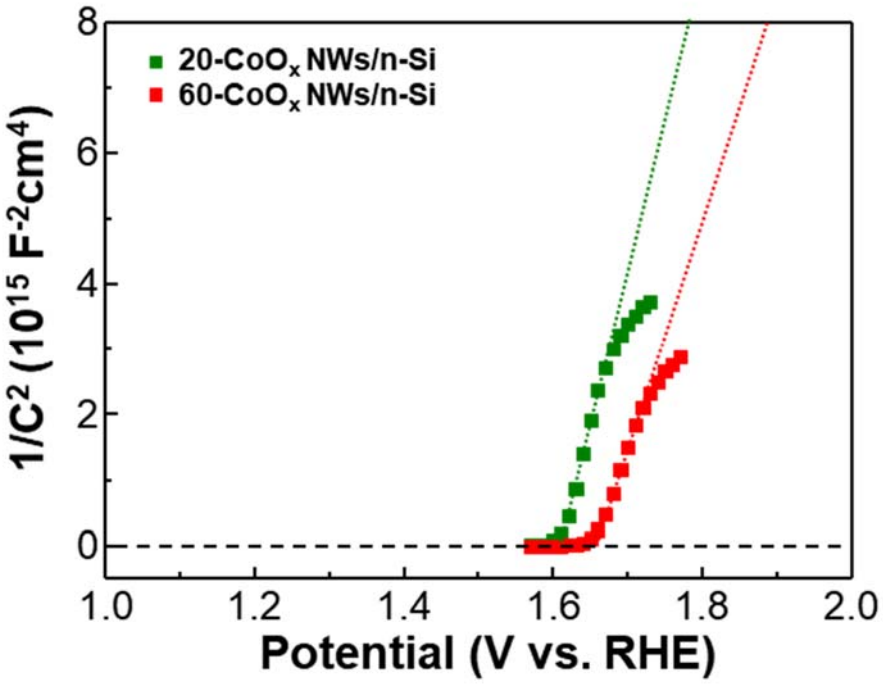

Figure S11. Mott-Schottky plots of 20-CoO_x NWs/n-Si and 60-CoO_x/n-Si in the 1 M NaOH electrolyte under light-off condition.

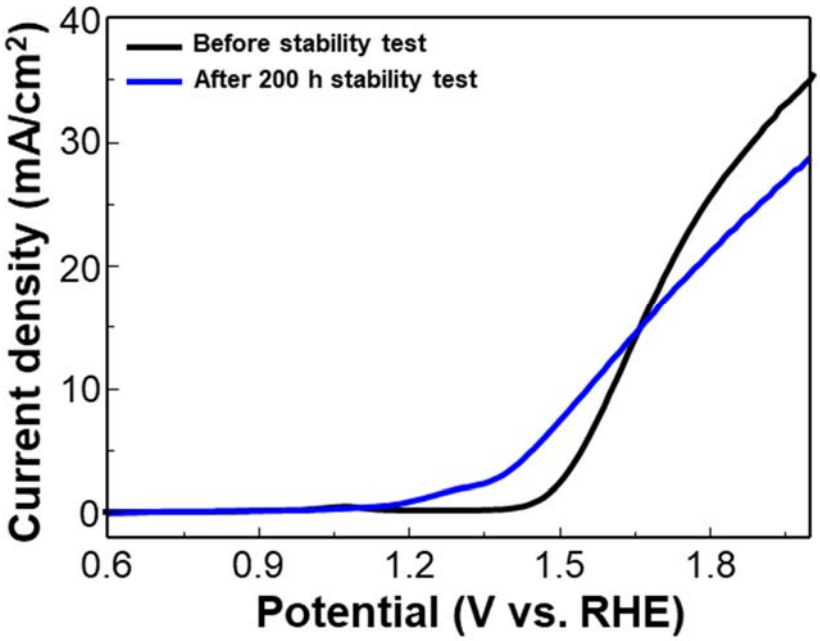

Figure S12. Linear sweep voltammogram of 10-CoO_x NWs/n-Si at a scan rate of 40 mV/s in the 1 M K-borate electrolyte before and after stability test.

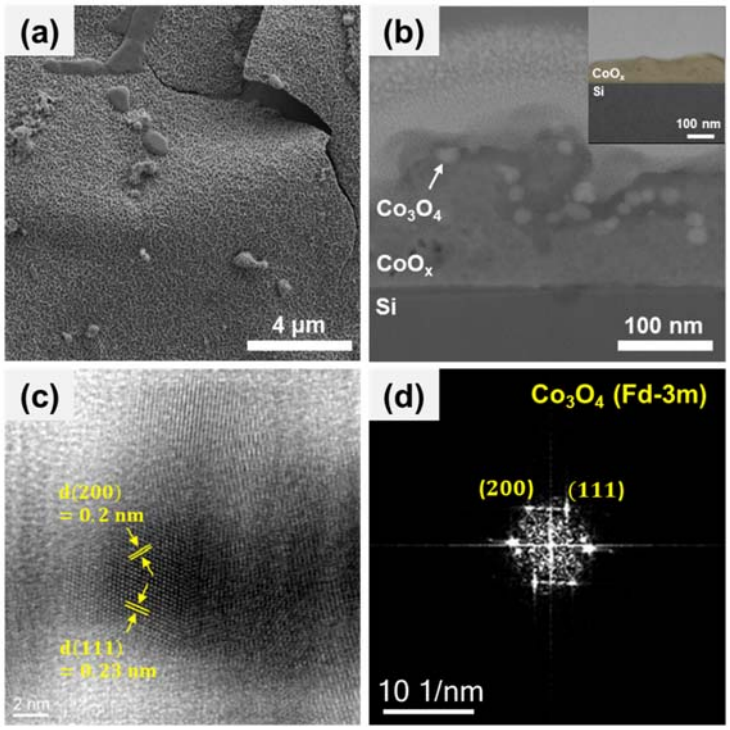

Figure S13. (a) FESEM and (b) Cross-sectional TEM of 10-CoO_x NWs/n-Si after stability test for 200 h. The inset shows TEM image of 10-CoO_x NWs/n-Si before stability test**.** (c) HRTEM images and (d) Electron diffraction pattern of 10-CoO_x NWs/n-Si after stability test for 200 h.

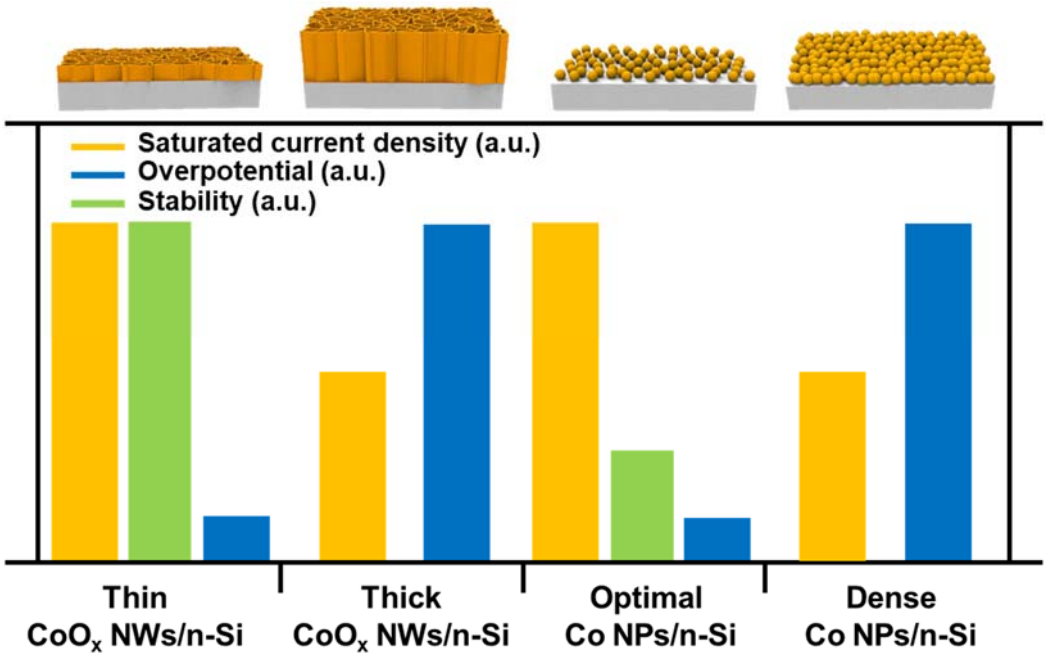

Figure S14. Schematics and PEC performances of morphology-controlled Co-based catalysts on the Si photoanodes.

Table S1. Fitted charge transfer resistances.

Photoanodes	$R_{ct,1}$ ($\Omega \cdot cm^2$)	$R_{ct,2}$ ($\Omega \cdot cm^2$)	$R_{ct,2}$ ($\Omega \cdot cm^2$)
	Contact/n-Si	n-Si/CoO_x NWs	CoO_x NWs/electrolyte
10-CoO_x NWs/n-Si	0.19	3.07	9.63
20-CoO_x NWs/n-Si	0	2.81	61.49
60-CoO_x NWs/n-Si	0	9.03	1529.32

Table S2. Fitted constant phase elements.

Photoanodes	CPE1-T	CPE2-P	CPE2-T	CPE2-P
10-CoO_x NWs/n-Si	1.59×10^{-7}	0.8095	8.57×10^{-4}	0.92489
20-CoO_x NWs/n-Si	1.722×10^{-8}	0.90263	6.25×10^{-4}	0.92332
60-CoO_x NWs/n-Si	7.49×10^{-9}	0.97729	1.61×10^{-3}	0.92985

Table S3.PEC performances of reported silicon photoanodes.

Photoanodes	**Stability**	**Current density at 1.23 V vs. RHE (mA/cm^2)**	**Saturated current density (mA/cm^2)**	**Onset potential (V vs. RHE)**	**Method**	**Ref.**
n-Si/SiO_x/CoO_x	12 h (1 M KOH)	3.5	32.5	-	ALD	1
n-Si/SiO_x/Co/CoOOH	25 h (Borate buffer)	-	35	-	Electrode position	2
n-Si/SiO_x/CoO_x	2500 h (1 M KOH)	22.9	30.2	1.02	ALD	3
n-Si/SiO_x/Ni@Co	100 h (1 M K-borate buffer)	10.65	36.7	1.02	Electrode position	4
b-Si/TiO_2/$Co(OH)_2$	4 h (1 M NaOH)	-	32.3	1.16	ALD, Electrode position	5
p^+n-Si/CoO_x	72 h (1 M NaOH)	30.8	37.5	<1	PE-ALD	6
p^+n-Si/CoO_x	24 h (1 M KOH)	17	30	-	ALD	7
n-Si/CoO_x (this work)	**200 h (1 M K-borate)**	**23.3**	**32.7**	1.06	**Electrode position**	-

PE-ALD: plasma-enhanced atomic layer deposition

Supporting Information References

(1) Oh, S.; Jung, S.; Lee, Y. H.; Song, J. T.; Kim, T. H.; Nandi, D. K.; Kim, S. H.; Oh, J. Hole-Selective $CoO_x/SiO_x/Si$ Heterojunctions for Photoelectrochemical Water Splitting. *ACS Catal.* **2018**, *8*, 9755–9764.

(2) Hill, J. C.; Landers, A. T.; Switzer, J. A. An Electrodeposited Inhomogeneous Metal-Insulator-Semiconductor Junction for Efficient Photoelectrochemical Water Oxidation. *Nat. Mater.* **2015**, *14*, 1150–1155.

(3) Zhou, X.; Liu, R.; Sun, K.; Papadantonakis, K. M.; Brunschwig, B. S.; Lewis, N. S. 570 mV Photovoltage, Stabilized n-Si/CoO_x Heterojunction Photoanodes Fabricated Using Atomic Layer Deposition. *Energy Environ. Sci.* **2016**, *9*, 892–897.

(4) Chen, J.; Xu, G.; Wang, C.; Zhu, K.; Wang, H.; Yan, S.; Yu, Z.; Zou, Z. High-Performance and Stable Silicon Photoanode Modified by Crystalline Ni@ Amorphous Co Core-Shell Nanoparticles. *ChemCatChem* **2018**, *10*, 5039–5045.

(5) Yu, Y.; Zhang, Z.; Yin, X.; Kvit, A.; Liao, Q.; Kang, Z.; Yan, X.; Zhang, Y.; Wang, X. Enhanced Photoelectrochemical Efficiency and Stability Using a Conformal TiO_2 Film on a Black Silicon Photoanode. *Nat. Energy* **2017**, *2*, 17045.

(6) Yang, J.; Cooper, J. K.; Toma, F. M.; Walczak, K. A.; Favaro, M.; Beeman, J. W.; Hess, L. H.; Wang, C.; Zhu, C.; Gul, S.; Yano, J.; Kisielowski, C.; Schwartzberg, A.; Sharp, I. D.; A Multifunctional Biphasic Water Splitting Catalyst Tailored for Integration with High-Performance Semiconductor Photoanodes. *Nat. Mater.* **2016**, *16*, 335–341.

(7) Yang, J.; Walczak, K.; Anzenberg, E.; Toma, F. M.; Yuan, G.; Beeman, J.; Schwartzberg, A.; Lin, Y.; Hettick, M.; Javey, A.; Ager, J. W.; Yano, J.; Sharp, I. D.; Efficient and Sustained Photoelectrochemical Water Oxidation by Cobalt Oxide/Silicon Photoanodes with Nanotextured Interfaces. *J. Am. Chem. Soc.* **2014**, *136*, 6191–6194.